# Electronic Supplementary information

**Mixed valence Sn doped $(CH_3NH_3)_3Bi_2Br_9$ produced by mechanochemical synthesis**

Xiaohan Jia,[1] Yuhan Liu,[1,2] Robin Perry,[2,3] Ivan P. Parkin,[1] Robert G. Palgrave[1]*

1. Department of Chemistry, University College London, 20 Gordon Street, London, WC1H 0AJ

2. London Centre for Nanotechnology and Department of Physics and Astronomy, University College London, London WC1E 6BT, United Kingdom

3. ISIS neutron spallation source, Rutherford Appleton Laboratory (RAL), Harwell Campus, Didcot OX11 0QX, United Kingdom

## Characterization

**Powder X-ray diffraction (PXRD)** patterns were measured on a Stoe STADI-P diffractometer (50 kV, 30 mA) using monochromated (Mo Kα1, 0.70930 Å) X-ray sources in transmission geometry with a STOE Dectris Mythen 1k detector. 2θ values ranging from 2.0° to 40.1° in steps of 0.5° at 10.0 s/step.

**X-ray photoelectron spectroscopy (XPS)** data were collected on a Thermo Scientific K-alpha photoelectron spectrometer with a monochromatic Al Kα radiation (photon energy of 1486.6 eV, 72 W 400 μm X-ray spot size). CasaXPS software was used to process the XPS data with the charge correction based on the adventitious carbon C 1s at 284.8 eV. The Shirley background was applied for peak area measurements. Multiple analysis points were collected for each sample to calculate the homogeneity of each compound.

The Sn Auger parameter was calculated following the work of Felix *et al.* [REF 45 in main text]. We calculate $a^*_{Sn} = BE_{XPS} + KE_{XAES}$ using the Sn $3d_{3/2}$ coreline, and the Sn $M_4N_{4,5}N_{4,5}$ X-ray induced Auger line. Values are compared with Sn oxide and oxyhalide samples discussed in reference 45.

**The UV-Vis optical spectra** for microcrystals were conducted on a Shimadzu UV-2600 spectrometer with two external detectors in diffuse reflectance mode (λ = 200-1400 nm, slit width = 5 nm). A barium sulfate pellet was used as the reflecting reference. The Kubelka-Munk relationship equation: $F(R) = (1-R)^2/2R$ was applied to convert the reflectivity (R) into absorbance (A).

**Table S1** Nominal and measured (XPS) percentage of Sn in $MA_3(Sn_xBi_{(1-x)})_2Br_9$ prepared by simple room temperature doping and after 200 °C heating, calculated from XPS core-level spectra.

| Theoretical Sn concentration | Measured Sn concentration (XPS) | |
|---|---|---|
| | room temperature | after annealing 200 °C |
| 0% | 0% | 0% |
| 1% | 7.0% | 3.0% |
| 25% | 31.1% | 23.4% |
| 30% | 38.6% | 36.0% |
| 40% | 31.0% | 42.1% |
| 50% | 51.6% | 47.8% |
| 60% | 60.6% | 60.3% |

$SnBr_2 + MA_3Bi_2Br_9$


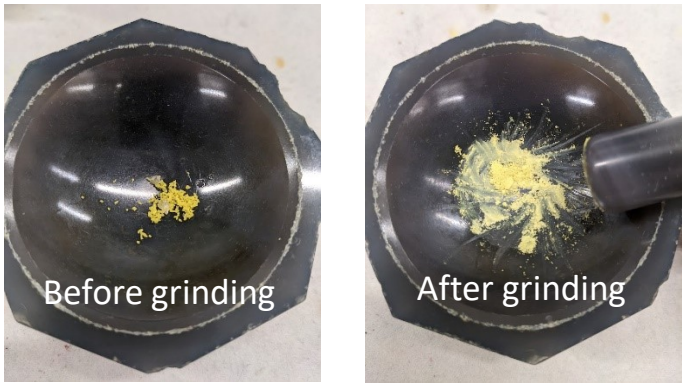


$SnBr_4 + MA_3Bi_2Br_9$

**Figure S1** Colour change of the room temperature mechanochemical doping reaction of the yellow $MA_3Bi_2Br_9$ (top left), the mixture of white $SnBr_2$ powder and $MA_3Bi_2Br_9$ before grinding (top centre) and the final product after grinding (top right). Bottom row, the same procedure with $SnBr_4$ instead of $SnBr_2$ yields no colour change.

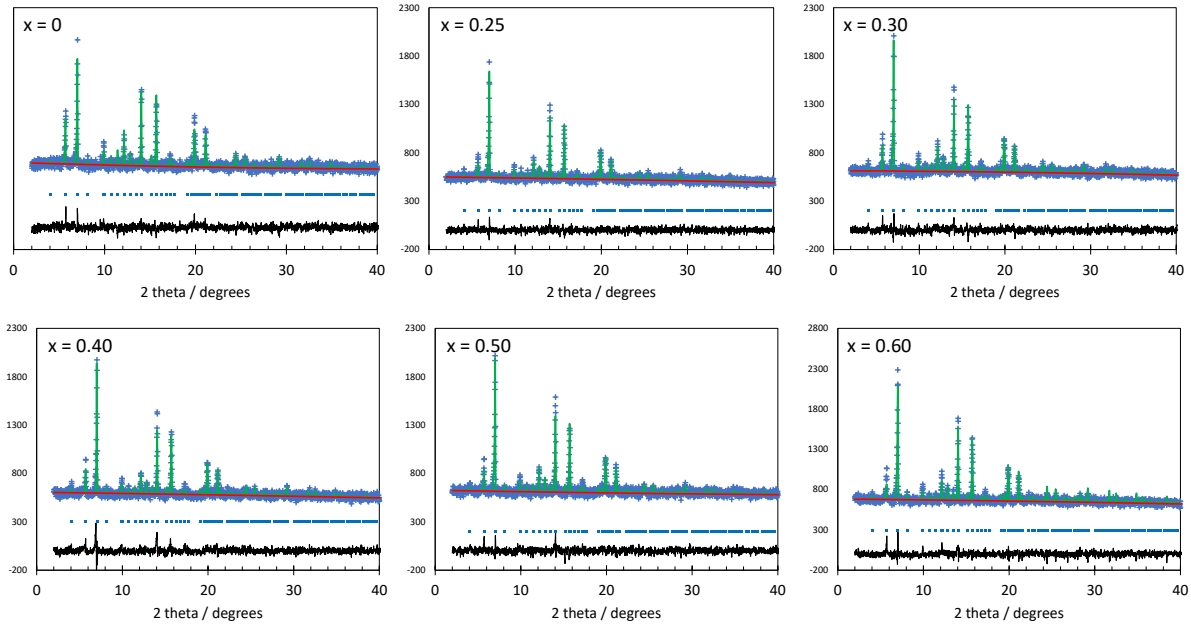


**Figure S2** Powder XRD patterns of $MA_3(Sn_xBi_{(1-x)})_2Br_9$ after annealing at 200°C in air.

**Table S2**. Refined lattice parameters from $MA_3(Sn_xBi_{(1-x)})_2Br_9$ samples after annealing at 200°C in air.

| x | A / Å | C / Å | V / Å$^3$ |
|---|---|---|---|
| 0 | 8.2124(28) | 10.0106(27) | 584.70(12) |
| 0.01 | 8.2144(19) | 10.0130(27) | 585.13(13) |
| 0.25 | 8.2080(21) | 10.0043(31) | 583.71(11) |
| 0.3 | 8.2140(18) | 10.0047(26) | 584.57(11) |
| 0.4 | 8.2113(18) | 10.0024(22) | 584.06(19) |
| 0.5 | 8.2106(18) | 10.0038(27) | 584.05(19) |
| 0.6 | 8.2069(14) | 9.9962(22) | 583.08(10) |

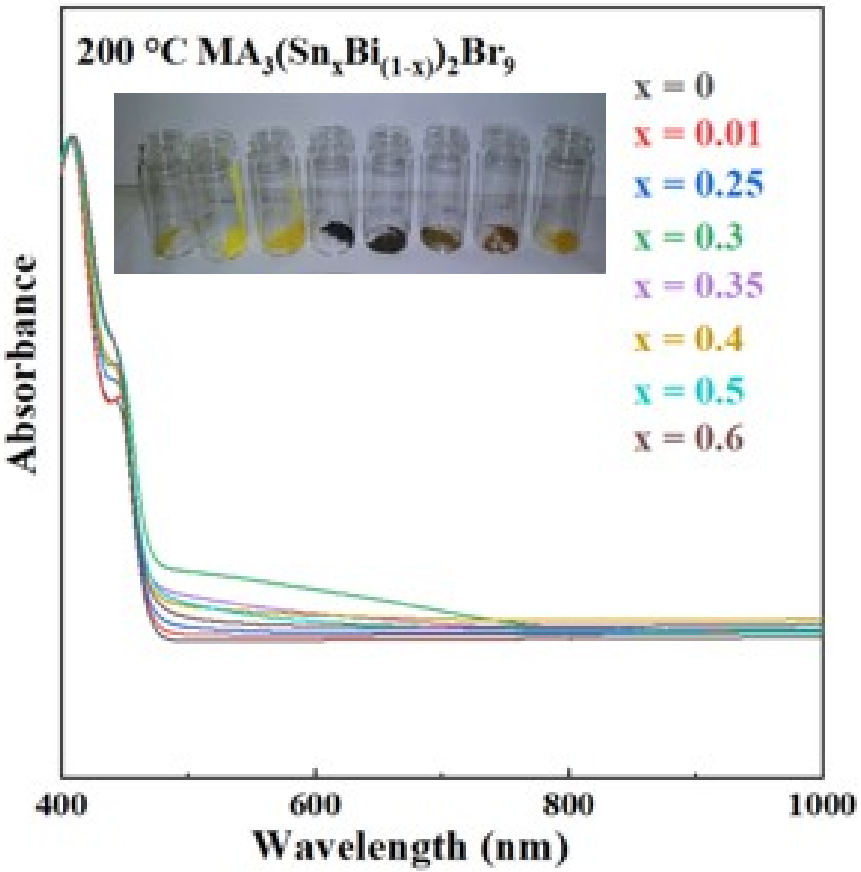


**Figure S3.** UV – vis absorption of $MA_3(Sn_xBi_{(1-x)})_2Br_9$ after annealing at 200°C in air. Inset, photograph of the samples with increasing x from left to right. Samples with x=0.3 retain the black colour even after annealing.

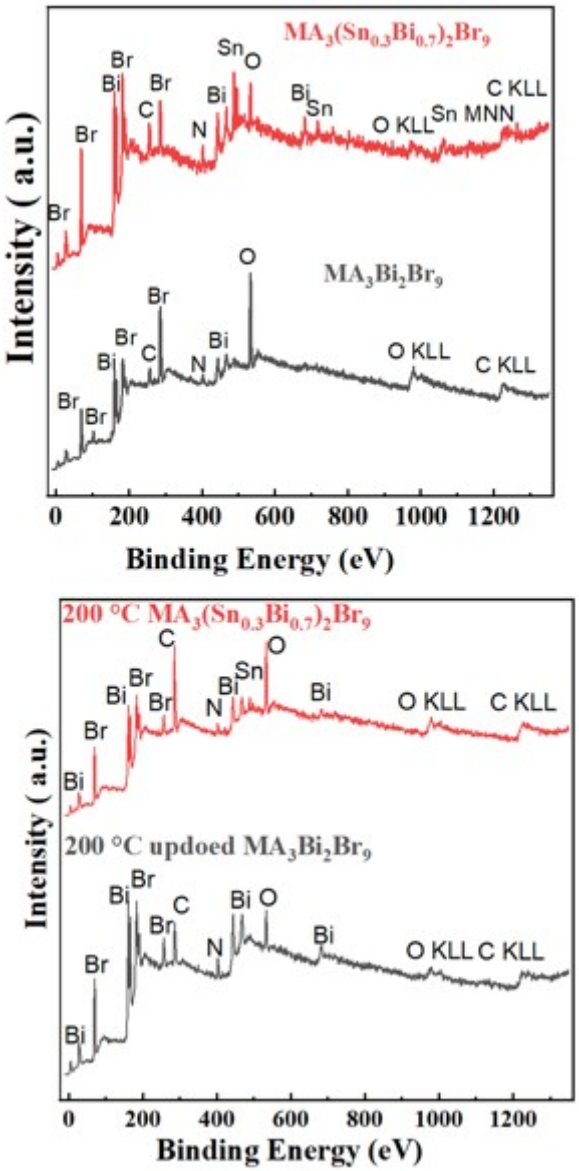


**Figure S4.** Survey XPS spectra of Sn:$MA_3Bi_2Br_9$ before (top) and after (bottom) 200°C air annealing.

(a)

(b)

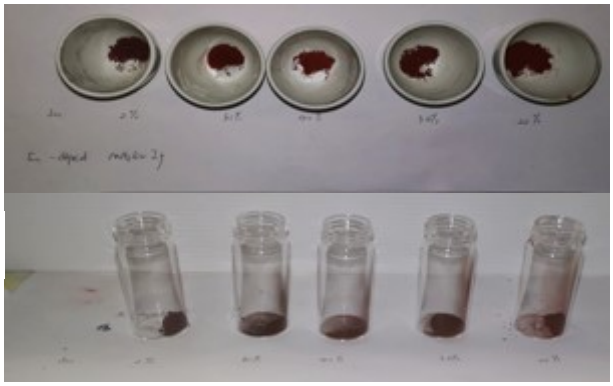

**Figure S5** Observation of Sn-doped $MA_3(Sn_xBi_{(1-x)})_2I_9$, where x = 0, 0.2, 0.3, 0.4, 0.5, prepared by mechanochemical reaction **(a)** at room temperature in air, **(b)** further heated in air at 200 °C for two hours after room temperature grinding.

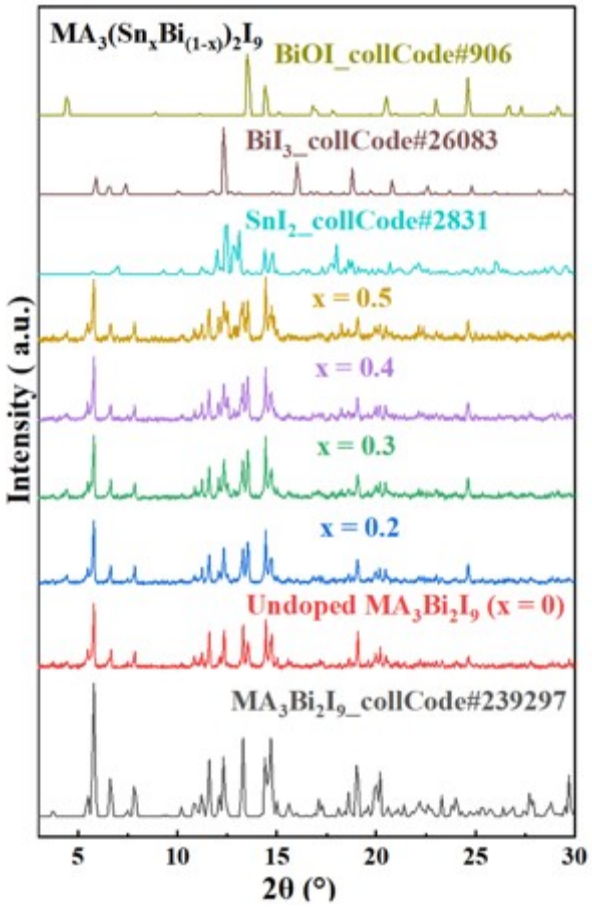


**Figure S6** Powder XRD patterns of room temperature Sn-doped $MA_3(Sn_xBi_{(1-x)})_2I_9$ where x = 0, 0.2, 0.3, 0.4, 0.5, compared with standard patterns of $MA_3Bi_2I_9$ and potential impurities including dopant $SnI_2$ and potential by-products of $BiI_3$ and BiOI.

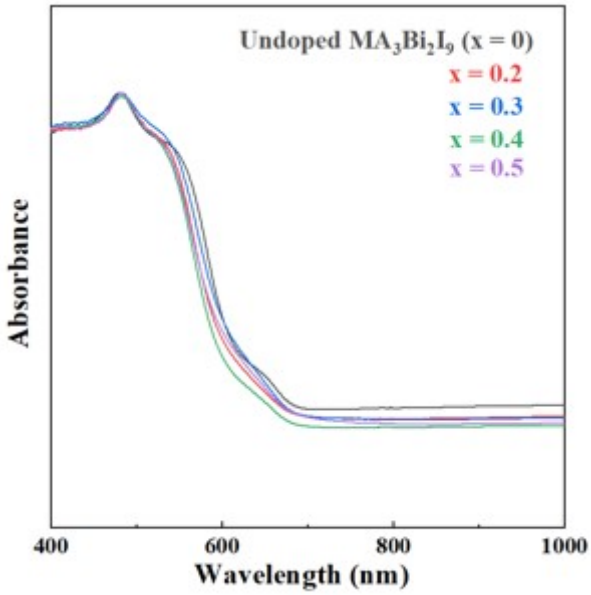

**Figure S7** UV-Vis absorption spectra of $MA_3(Sn_xBi_{(1-x)})_2I_9$ prepared by room temperature mechanochemical reaction, where x = 0, 0.2, 0.3, 0.4, 0.5.

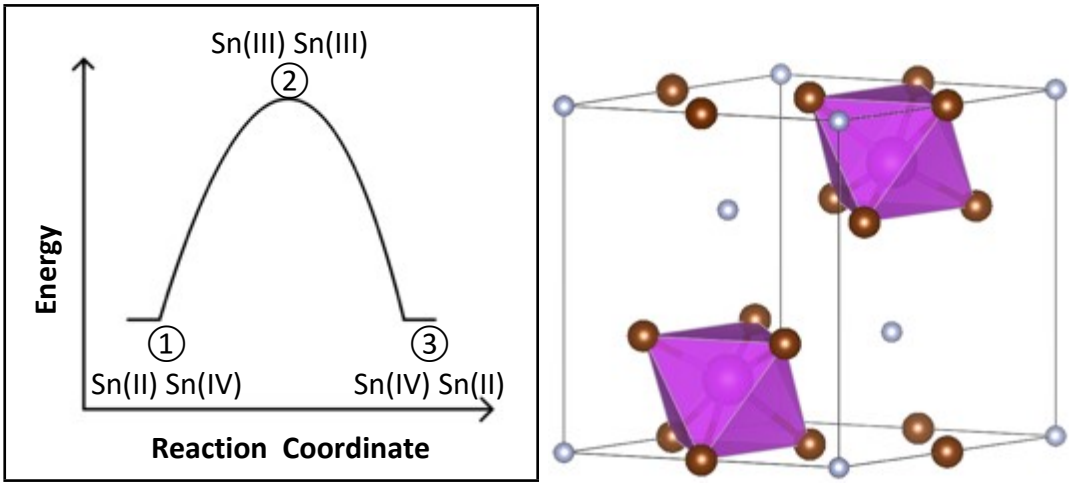


**Figure S8** (a) Energy profile diagram of Sn(II) to Sn(IV) IVCT mechanism. (b) Structure of $MA_3Bi_2Br_9$

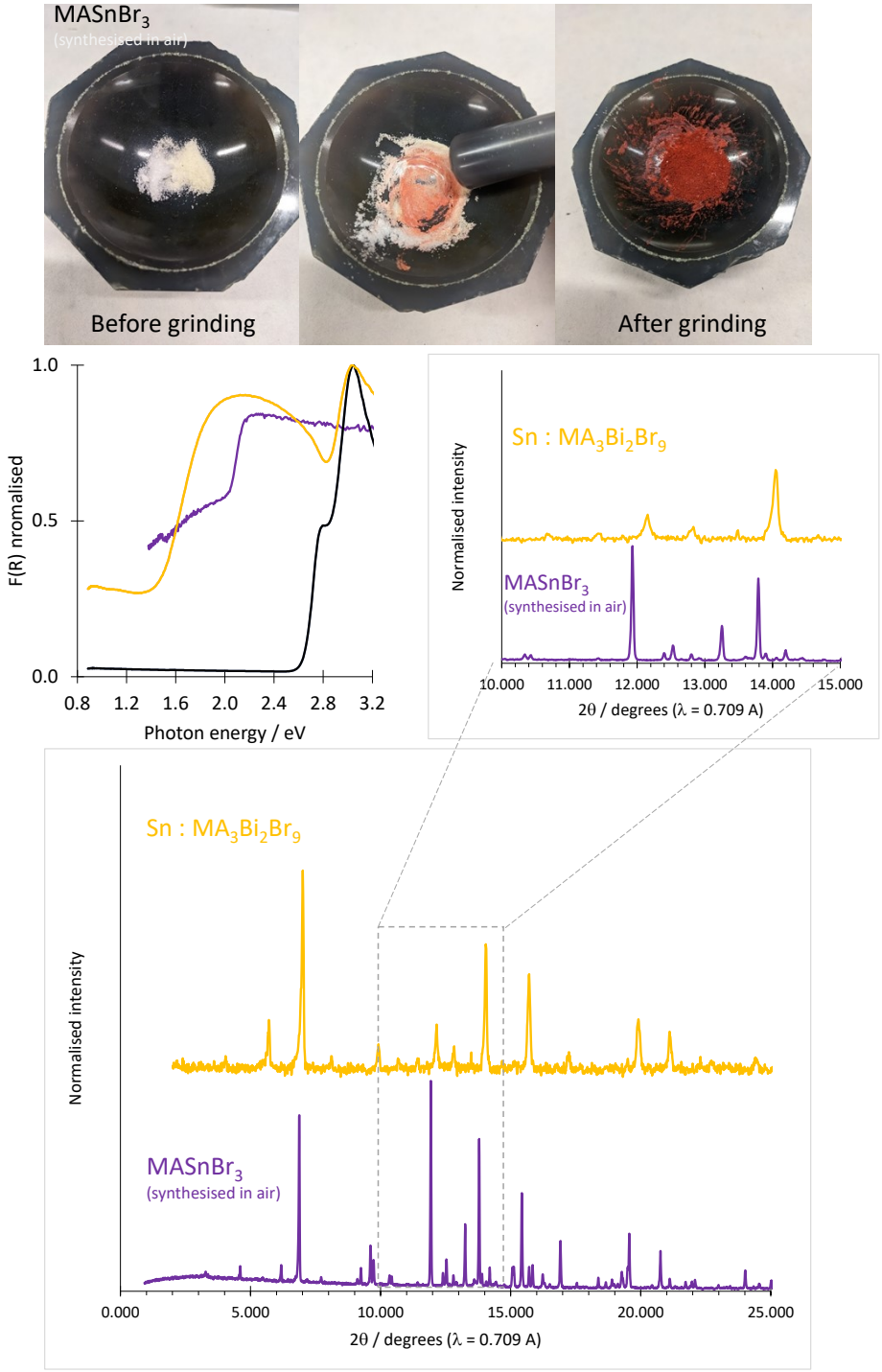


**Figure S9**. Top, three photographs taken during the mechanochemical reaction between MABr and $SnBr_2$. The XRD pattern (bottom) shows peaks corresponding to $MASnBr_3$, as well as some small unidentified peaks likely due to decomposition in air. The optical spectrum of the red MASnBr3 powder is shown in the centre left panel, in comparison with the undoped $MA_3Bi_2Br_9$ (black) and Sn $MA_3Bi_2Br_9$ (yellow)

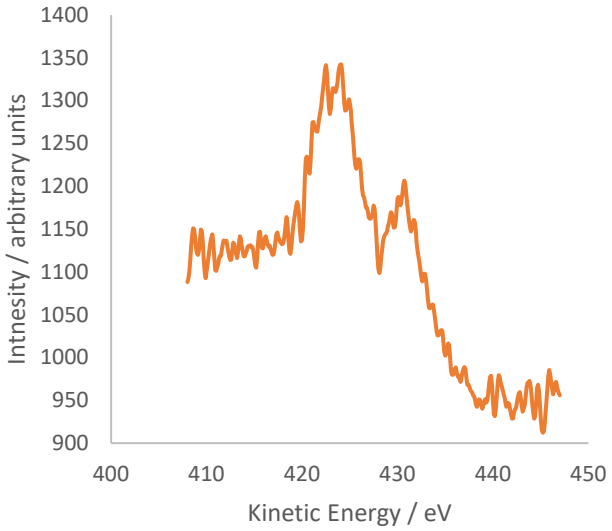


Figure S10. Sn MNN X-ray excited Auger spectrum from Sn: $MA_3Bi_2Br_9$